# Fibroblasts Isolated from Common Sites of Breast Cancer Metastasis Enhance Cancer Cell Growth Rates and Invasiveness in an Interleukin-6–Dependent Manner

Adam W. Studebaker,[1] Gianluca Storci,[5,6] Jillian L. Werbeck,[2] Pasquale Sansone,[5,7] A. Kate Sasser,[1,3] Simona Tavolari,[8] Tim Huang,[4] Michael W.Y. Chan,[9] Frank C. Marini,[10] Thomas J. Rosol,[2] Massimiliano Bonafé,[5,6] and Brett M. Hall[1,3]

[1]Center for Childhood Cancer, Children's Research Institute; [2]Department of Veterinary Biosciences, College of Veterinary Medicine, [3]Integrated Biomedical Science Graduate Program, Department of Pediatrics, School of Medicine and Public Health, and [4]Department of Molecular Virology, Immunology, and Medical Genetics, Comprehensive Cancer Center, The Ohio State University, Columbus, Ohio; [5]Center for Applied Biomedical Research, St. Orsola-Malpighi University Hospital, [6]Department of Experimental Pathology, [7]Department of Pharmacology and Toxicology, and [8]Departments of Experimental and Evolutionary Biology, University of Bologna, Bologna, Italy; [9]Department of Life Science, National Chung Cheng University, Chia-Yi, Taiwan, Republic of China; and [10]Department of Blood and Bone Marrow Transplantation, University of Texas M. D. Anderson Cancer Center, Houston, Texas

## Abstract

**Common sites of breast cancer metastasis include the lung, liver, and bone, and of these secondary metastatic sites, estrogen receptor α (ERα)–positive breast cancer often favors bone. Within secondary organs, cancer cells would predictably encounter tissue-specific fibroblasts or their soluble factors, yet our understanding of how tissue-specific fibroblasts directly affect cancer cell growth rates and survival remains largely unknown. Therefore, we tested the hypothesis that mesenchymal fibroblasts isolated from common sites of breast cancer metastasis provide a more favorable microenvironment with respect to tumor growth rates. We found a direct correlation between the ability of breast, lung, and bone fibroblasts to enhance ERα-positive breast cancer cell growth and the level of soluble interleukin-6 (IL-6) produced by each organ-specific fibroblast, and fibroblast-mediated growth enhancement was inhibited by the removal or inhibition of IL-6. Interestingly, mice coinjected with MCF-7 breast tumor cells and senescent skin fibroblasts, which secrete IL-6, developed tumors, whereas mice coinjected with presenescent skin fibroblasts that produce little to no IL-6 failed to form xenograft tumors. We subsequently determined that IL-6 promoted growth and invasion of breast cancer cells through signal transducer and activator of transcription 3–dependent up-regulation of Notch-3, Jagged-1, and carbonic anhydrase IX. These data suggest that tissue-specific fibroblasts and the factors they produce can promote breast cancer disease progression and may represent attractive targets for development of new therapeutics.** [Cancer Res 2008;68(21):9087–95]

## Introduction

Metastasis is the single greatest cause of morbidity and mortality in cancer patients, and the observation that bone and visceral organs represent the primary sites of metastasis in women with breast cancer was first published over a century ago (1). In that seminal publication, Paget proposed that breast cancer cells "seed" tissues of metastasis, "the soil," and that each must contribute to the predictable frequency of organ-specific metastasis. Although much progress has recently been made with respect to tumor cell–specific gene profiles that predict organ-specific metastasis (2), it is less clear whether specific organs harbor inherent biological characteristics that make secondary sites more attractive than others during breast cancer metastasis. Human clinical data and genetic mouse models of breast cancer indicate that breast carcinomas have a strong metastatic predilection for lung and bone, with estrogen receptor α (ERα)–positive tumor cells favoring bone as their first site of distant metastasis and ERα-negative tumor cells favoring visceral organs (2–6).

Fibroblastic stromal cells have been linked to several activities that promote tumor growth and metastasis. These activities include angiogenesis (7), epithelial to mesenchymal transition (8), progressive genetic instability (9, 10), deregulation of antitumor immune responses (11), enhanced metastasis (12), and enhanced growth (13, 14). However, many of the underlying mechanisms that account for these observations remain poorly defined. There are many attributes of fibroblast biology that contribute to this gap in knowledge, some of which include the inherent complexity of fibroblast behavior within *in vivo* tumor microenvironments, the paucity of available *in vitro* models that effectively reproduce *in vivo* tumor-stroma interactions, and the inherent diversity of human fibroblasts (15–19). Nevertheless, a growing number of studies indicate that tissue-specific fibroblasts are influential players in the progression of metastatic cancer (20), and senescent fibroblasts have been shown to promote *in vitro* invasiveness and growth of neoplastic cells in xenografts (21–23). Taken together, these data suggest that organ-specific fibroblasts can contribute to promote tumor progression and that inherent tumor-promoting abilities may increase with advancing age.

Recently, Yashiro and colleagues (16) showed that human breast fibroblasts but not skin fibroblasts enhanced the growth rates of primary breast carcinoma xenografts *in vivo*. In addition, Karnoub and colleagues (12) showed that bone fibroblasts enhanced the

**Note:** Supplementary data for this article are available at Cancer Research Online (http://cancerres.aacrjournals.org/).

A.W. Studebaker and G. Storci contributed equally to this work.

**Requests for reprints:** Brett M. Hall, Center for Childhood Cancer, WA5015, Nationwide Children's Hospital, 700 Children's Drive, Columbus, OH 43205. Phone: 614-355-2650; Fax: 614-722-5895; E-mail: hall.125@osu.edu or Massimiliano Bonafé, Department of Experimental Pathology, University of Bologna, Via S. Giacomo 12, 40126 Bologna, Italy. Phone: 39-051-636-4009; Fax: 39-051-636-3902; E-mail: massimiliano.bonafe@unibo.it.



doi:10.1158/0008-5472.CAN-08-0400

growth rate of MCF-7 (ERα positive) but not MDA-MB-231 (ERα negative) tumor xenografts *in vivo*. However, a mechanistic explanation for these *in vivo* data from both studies remains unresolved. We recently showed that interleukin-6 (IL-6) is a potent growth factor for ERα-positive breast cancer in both three-dimensional (3D) matrix-based proliferation assays and *in vivo* (13). Given these data and the fact that cancer has a propensity to metastasize to specific organs (24), we examined the direct effect of a panel of organ-specific fibroblasts on breast tumor cell growth rates and invasion.

The context in which fibroblasts and tumor-stroma interactions are examined can greatly influence experimental outcomes, especially when moving from two-dimensional (2D) tissue culture to 3D tissue culture and animal model systems (13, 15, 25, 26). For example, cancer cell gene expression profiles (26), fibroblast cell behavior (25), and cancer cell response to mitogenic factors (27) can vary dramatically depending on the dimensionality and complexity of the experimental environment used. Although many biological correlations are often found when comparing 3D *in vitro* and *in vivo* systems, large deviations with respect to tumor cell gene expression profiles and tumor-stroma interactions are commonly observed between 2D and 3D or *in vivo* systems (13, 15, 26). We recently developed a 3D *in vitro* tumor growth assay (TGA), which better replicates the dimensionality and some of the complexities associated with *in vivo* tumor microenvironments (12, 13). The 3D TGA can be used as a noninvasive 3D proliferation assay to evaluate the effect of tissue-specific fibroblasts or their soluble factors on tumor cell growth rates *in vitro* with strong correlations to *in vivo* outcomes (12, 13, 28). In line with these findings, multicellular spheroids grown under low attachment conditions have also proven to be an invaluable 3D model to study properties of breast cancer cells that are difficult to ascertain in standard 2D culture conditions (29, 30).

The pleiotropic cytokine IL-6 has many homeostatic functions, including roles in B-cell development, myeloid lineage maturation, acute phase immune responses, hepatic function, and bone absorption (31). Multiple studies have established IL-6 as a potent growth factor for several cancers, including multiple myeloma (32), prostate cancer (33), cholangiocarcinoma (34), and breast cancer (13, 14). Furthermore, the oncogenic capacity of Ras has recently been linked to induction of IL-6 gene expression, which in turn promotes angiogenesis and growth in mesenchymal and epithelial cell types, including mammary epithelial cells (35). With respect to breast cancer, elevated IL-6 serum levels are known to correlate with disease staging and unfavorable clinical outcomes in women with metastatic disease (36, 37). Signal transducer and activator of transcription 3 (STAT3) is one of the primary intracellular targets that is activated following exposure to IL-6 (31), and STAT3 activity correlates with enhanced tumor cell growth, survival, and immune evasion in breast cancer (13, 38–40).

Our current data suggest that IL-6 represents a biological link between organ-specific mesenchymal fibroblasts and enhanced growth rates of breast cancer cells. Fibroblasts, isolated from organs associated with breast cancer invasion and metastasis (i.e., breast, lung, and bone), produced elevated levels of IL-6 when exposed to tumor-derived microenvironments and, in turn, each enhanced breast cancer growth rates. Among the complex array of soluble factors produced by fibroblasts, the presence of soluble IL-6 was indispensable for support of enhanced breast cancer cell growth rates. In contrast, skin fibroblasts and endothelial cells produced little to no IL-6 and correspondingly had little effect on breast cancer cell growth rates. Our findings support the postulate that breast cancer cells, which produce little to no autocrine IL-6 (e.g., ERα-positive tumor cells; ref. 13), have a growth advantage in sites that provide paracrine IL-6 from organ-specific fibroblasts. Bone is one of the few tissues that maintain elevated IL-6 levels under noninflammatory conditions (41), and recent clinical data have shown that primary ERα-positive breast tumors contain significantly less IL-6 than ERα-negative breast tumors (42).

## Materials and Methods

**Breast epithelial and cancer cell lines.** MDA-MB-231 ($ER\alpha^-$; $IL\text{-}6^+$), MCF-7 ($ER\alpha^+$; $IL\text{-}6^-$), BT474 ($ER\alpha^+$; $IL\text{-}6^-$), and MCF-10A (immortalized $ER\alpha^-$ mammary epithelia) cell lines were purchased from the American Type Culture Collection (ATCC). All lines were maintained in humidified incubators at 37°C and 5% $CO_2$. The breast cancer cell lines MDA-MB-231, MCF-7, and BT474 were cultured in RPMI 1640 containing 10% characterized fetal bovine serum (FBS; HyClone), 2 mmol/L L-glutamine, 10 units/mL penicillin, and 10 μg/mL streptomycin. The immortalized breast epithelial cell line MCF-10A was cultured in Ham's F12 containing 5% characterized FBS, 2 mmol/L L-glutamine, 10 units/mL penicillin, 10 mg/mL streptomycin, 5 mg/mL insulin (Sigma), 1 mg/mL hydrocortisone (Sigma), 10 ng/mL epidermal growth factor (Sigma), and 100 mg/mL cholera toxin (Sigma).

**Nonbreast fibroblast cells and endothelial cells.** MRC-5 (normal human lung embryonic fibroblast), WI-38 (normal human lung embryonic fibroblast), WS-1 (normal human skin embryonic fibroblast), CCD-39sk (normal human skin fibroblast), and human umbilical vein endothelial cells were all purchased from ATCC. MRC-5, WI-38, WS-1, and CCD-39sk were cultured in RPMI 1640 with 10% characterized FBS as described above for breast cancer cell lines. Human bone marrow stromal cells Ped300, P162, P163, and P164 were obtained from Dr. Laura Gibson (West Virginia University, Morgantown, WV). Human bone marrow fibroblasts were maintained in α-MEM containing 10% defined FBS, 2 mmol/L L-glutamine, 10 units/mL penicillin, and 10 μg/mL streptomycin. The primary human MSC (hMSC-02) cell line was obtained from Dr. Darwin Prockop's group at Tulane University (New Orleans, LA).[11] Primary skin fibroblasts were obtained from a 37-y-old woman and cultured as previously described (14). All experiments were performed between sixth and ninth passages of culture. Long-term exposure of skin fibroblasts to IL-6 was performed as follows: nonsenescent passage 6 dermal fibroblasts were split into two subcultures, one was kept in the absence and the other in the presence of IL-6 (10 ng/mL), which were replaced every 3 d at the time of culture medium change. No senescence-associated biochemical changes [β-galactosidase activity and senescence-associated heterochromatic foci (SAHF)] were observed during the first 2 wk of culture.

**Isolation of fibroblasts from normal and cancer breast tissue.** Normal breast tissues from reduction mammoplasties or from ductal breast carcinoma patients ($n$ = 2, normal and tumor tissue pairs) were minced with scalpels in a tissue culture dish and then enzymatically dissociated in 5 mL of mammary epithelial growth medium (Cambrex) supplemented with 2% bovine serum albumin (Fraction V, Fisher Scientific), 10 ng/mL cholera toxin, 300 units/mL collagenase (Invitrogen), and 100 units/mL hyaluronidase (Calbiochem) at 37°C for 18 h. All tissues were obtained from the Cooperative Human Tissue Network with Institutional Review Board approval or from ductal breast carcinoma patients with approval of the local ethical committee and by the patient's written informed consent (Bologna, Italy).

On the second day, the suspension was centrifuged at 700 rpm ($80 \times g$) for 4 min to separate the epithelial and fibroblast cells. Fibroblast cells in the supernatant were pelleted by centrifugation at 800 rpm ($100 \times g$) for 10 min followed by two washes with DMEM/F12 medium. The cell pellet

[11] http://www.som.tulane.edu/gene_therapy/distribute.shtml

was resuspended in DMEM/F12 medium supplemented with 5% FBS (Invitrogen) and 5 μg/mL insulin and plated in 25 $cm^2$ tissue culture flasks. The cultures were incubated undisturbed for 2 to 3 d at 37°C at 5% $CO_2$.

**2D and 3D serum-free fibroblast conditioned medium.** Fibroblast conditioned medium (Fibro-CM) was prepared from fibroblasts grown in either a 2D (2D Fibro-CM) or 3D (3D Fibro-CM) *in vitro* environment. To generate a 3D *in vitro* environment, 0.5 mL of a 6 mg/mL Cultrex basement membrane extract (BME; Trevigen, Inc.) solution was added to six-well plates. Subsequently, $1.0 \times 10^5$ cells were plated into the six-well plates containing BME and allowed to adhere overnight. The 2D *in vitro* environment was prepared by plating $1.0 \times 10^5$ cells directly into six-well plates. The following morning, all cells were washed thoroughly with 1× PBS, and fresh serum-free medium (phenol red–free RPMI 1640 supplemented with 2 mmol/L L-glutamine) was added to the cells. In addition, phenol red–free medium containing 5% FBS was added to a subset of cells grown in 2D. Cell cultures were incubated for 48 h and soluble supernatants were collected and 0.2 μm sterile filtered.

**Soluble IL-6 protein quantification.** Fibro-CM, prepared as indicated above, was assayed for IL-6 protein levels using the DuoSet Human IL-6 ELISA (R&D Systems). The IL-6 ELISA was performed according to the manufacturer's instructions. In addition, IL-6 was removed from a subset of Fibro-CM from 3D/Cultrex BME by IL-6 immunoprecipitation (see below).

**IL-6 immunoprecipitation.** IL-6 was immunoprecipitated as previously described (13) with one exception [i.e., 3D Fibro-CM was incubated with 2 μg/mL anti-IL-6 monoclonal antibody (Mab206; R&D Systems) for 4 to 6 h at 4°C with constant rotation]. To verify that IL-6 had been removed from the conditioned medium, an aliquot of conditioned medium stripped of IL-6 via immunoprecipitation was tested for IL-6 concentration by ELISA, and in all cases, IL-6 concentrations were >14-fold less as determined by IL-6 ELISA (Supplementary Fig. S1).

**Western blot analysis.** Breast tumor cells were plated in six-well plates at a concentration of 500,000 per well and allowed to adhere overnight. Cells were incubated in conditions indicated for 48 h. After treatment, cells were washed in PBS and lysed in SDS lysis buffer [62.5 mmol/L Tris-HCl, 2% (w/v) SDS, 10% glycerol, 50 nmol/L DTT, 0.01% (w/v) bromphenol blue]. Primary antibodies included anti-phosphorylated ($Tyr^{705}$) STAT3 (Cell Signaling), anti-actin (clone AC-15; Sigma), and anti-Notch-3 rabbit polyclonal (Santa Cruz Biotechnology). Secondary reagents included goat anti-rabbit horseradish peroxidase (HRP; Santa Cruz Biotechnology) and sheep anti-mouse HRP (Santa Cruz Biotechnology).

**Stable red fluorescent tumor cell lines.** Stable red fluorescent tumor cell lines were generated as described previously (13, 28). Briefly, stable monomeric DsRed MCF-7 and BT474 cell lines ($MCF\text{-}7^{VSVgR}$ and $BT474^{VSVgR}$) were generated using VSV-G pseudotyped murine leukemia virus (MLV) retrovirus containing the pRetroQ-DsRed Monomer C1 packaging construct (Clontech). Retrovirus was produced by cotransfecting pVSV-G and pRetroQ-DsRed into the PG2-293 MLV packaging cell line and collecting virus from cellular supernatants. MCF-7 cells that expressed stable monomeric DsRed were grown in 5 μg/mL puromycin and underwent two consecutive rounds of sterile cell sorting (i.e., $MCF\text{-}7^{VSVgR2}$ and $BT474^{VSVgR2}$) before use.

**3D TGA.** The 3D TGA is a fluorescence-based 3D *in vitro* proliferation assay that is designed to noninvasively monitor tumor cell growth for up to 10 to 12 d after cells are embedded in Cultrex BME at 3 mg/mL (13, 28). Briefly, red fluorescent $MCF\text{-}7^{VSVgR2}$ and $BT474^{VSVgR2}$ tumor cells were embedded in 3 mg/mL Cultrex BME in a black-walled, clear-bottom 96-well plate at 12,500 tumor cells (±) 3D Fibro-CM, 3D Fibro-CM(-IL-6) (i.e., 3D Fibro-CM with IL-6 removed via immunoprecipitation), or recombinant IL-6 (PeproTech), as indicated. Each experimental condition was set up in triplicate within a 100 μL plug of 3 mg/mL BME and then overlaid with phenol red–free, serum-free RPMI 1640. Individual well fluorescence intensities were monitored daily for 1 wk, and relative MCF-7 and BT474 growth rates were documented as relative fluorescence units and graphed as fold change (growth). For a more complete description of this assay and its utility for evaluating growth rate kinetics of breast cancer cells in complex 3D tumor-like microenvironments, see our previously published studies (13, 28).

***In vivo* tumorigenic assay.** Eighteen animals (6-wk-old female BALB/c nude mice; Charles River) were used for the *in vivo* tumorigenic assay. MCF-7 cells ($5 \times 10^5$) were s.c. injected [$\pm 1 \times 10^5$ fibroblasts of indicated origin (see text)] in the superior left or right dorsal area. The presence or

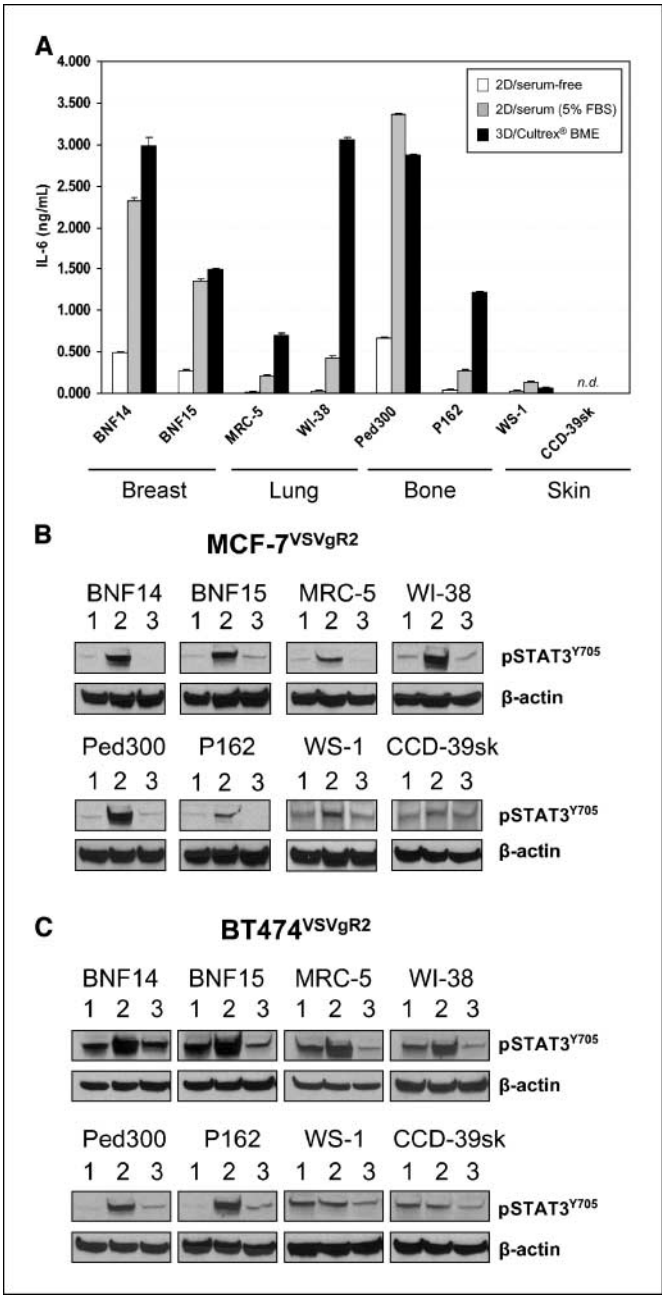


**Figure 1.** Conditioned media from breast, bone, and lung fibroblasts induced phosphorylation of STAT3 on $Tyr^{705}$ ($pSTAT3^{Y705}$) in an IL-6–dependent manner. *A,* organ-specific fibroblasts produce IL-6, which is influenced by 2D and 3D growth conditions. Fibroblasts were cultured in 2D (directly on plastic tissue culture dishes) or in 3D (on a thin layer of BME). Cells grown in 2D were cultured in serum-free TGA medium or identical medium containing 5% FBS. Cells cultured in 3D were grown in Cultrex BME with TGA medium (no FBS). Supernatants were harvested 48 h after addition of growth medium and assayed for IL-6 concentrations using an IL-6–specific ELISA. The experiment was performed in triplicate and is a representative of similar experiments. *n.d.,* none detected. Western blot analysis of $pSTAT3^{Y705}$ in $MCF\text{-}7^{VSVgR2}$ (*B*) or $BT474^{VSVgR2}$ (*C*) cells after exposure to serum-free TGA medium (*lane 1*), Fibro-CM (*lane 2*), or Fibro-CM stripped of IL-6 via immunoprecipitation (*lane 3*). Induction of $pSTAT3^{Y705}$ in breast cancer cells was negligible or absent following exposure to skin fibroblasts when compared with other organ-specific fibroblasts.

absence of tumor was assessed by visual inspection and palpation. Tumor volume was calculated every 3 d by measuring two perpendicular diameters and height. Anti-IL-6 antibody (100 μg per injection) was s.c. administered close to the tumor mass, every 3 d, starting from 5th wk, similarly to what had been recently described (35). Animals were euthanized at 8 wk after MCF-7 challenge, and tumors were resected and subjected to microscopic and macroscopic evaluation. All the procedures were previously approved by the local veterinary ethical committee.

**Boyden chamber invasion assay.** Cell invasion into Matrigel BME was assessed using Boyden chambers (New Technologies Group), containing a polyvinylpyrrolidone-free polycarbonate filter with 8-μm pores, coated with 15 μg of Matrigel BME (Sigma). MCF-7 cells ($1 \times 10^5$) were seeded in the upper chamber in serum-free medium ± IL-6 (10 ng/mL) or fibroblast supernatant [± anti-IL6 antibody (1.5 μg/mL)] for 1 h before running the invasion assay. The assay was also performed using MCF-7 cells stably infected with Notch-3–specific short hairpin RNA (shRNA) or transiently transfected with carbonic anhydrase IX (CA-IX)–specific small interfering RNA (siRNA). Complete medium was placed in the lower chamber as chemoattractant. Invasion assays were scored after 24 h at 37°C in humidified 5% $CO_2$ incubators. Noninvading cells were removed from the upper surface of the filters, and invading cells in the lower surface were fixed, stained with toluidine blue (Sigma), and scored as the mean number of invaded cells per four random optical fields at ×200 total magnification.

**Transient RNA interference and plasmid transfection.** siRNA directed against CA-IX and appropriate control RNA interference were purchased from Invitrogen. Transfection was performed with Lipofectamine 2000 (Invitrogen), and all transfections were performed when cells were ~60% confluent. Cells were assessed after 72 h of siRNA transfection as described previously (14).

MCF-7 cells stably infected with the pSuperPuro retroviral vector encoding Notch-3–specific shRNA have been previously described (14).

**Statistical analysis.** Probabilities for the Student's *t* test are listed as "$P(T \leq t)$ two-tail" with an $\alpha$ of 0.05. Unless otherwise indicated, all 3D TGA data represent "*n*" experiments with three averaged wells per individual experiment. Continuous variables (number of invading cells in Boyden chamber assays) were analyzed by ANOVA (unequal variance assumed). Post hoc test (unequal variance assumed) was used for greater than two-sample comparisons. Nonparametric tests (Mann-Whitney) were used for two-sample comparisons. Exact test (Fisher's test for rows × columns tables) was used for categorical analysis. *P* value of <0.05 was considered statistically significant for all tests. Statistical analysis was completed using Statistical Package for the Social Sciences 10.1 Package (SPSS), and Microsoft Office Excel (v.11.6560.6568 SP2) was used for data analysis involving regression or Student's *t* test: paired two sample for means.

## Results

**Organ-specific fibroblasts from breast, lung, and bone produce elevated levels of IL-6 when compared with skin fibroblasts.** To determine the amount of soluble IL-6 produced by eight human mesenchymal fibroblast lines (i.e., two fibroblast cell lines each from breast, lung, bone, and skin), each line was grown under three unique culture conditions (i.e., 2D/serum starvation, 2D/serum-containing medium, and 3D/BME). Supernatants from each fibroblast line were then collected and levels of soluble human IL-6 were quantified. Little to no IL-6 was produced by any of the eight fibroblast lines under 2D/serum starvation conditions (Fig. 1*A*). However, fibroblasts isolated from breast, lung, and bone produced 217 to 3,355 pg/mL and 705 to 3,061 pg/mL under 2D/serum cultures and on 3D/BMEs, respectively (Fig. 1*A*). In contrast, skin fibroblasts produced 0 to 140 pg/mL and 0 to 59 pg/mL under identical conditions (Fig. 1*A*).

**Paracrine IL-6 from organ-specific fibroblasts induces chronic STAT3 phosphorylation in breast cancer cells.** We recently reported that IL-6 was necessary and sufficient for bone marrow–derived mesenchymal stem cells (MSC) to chronically

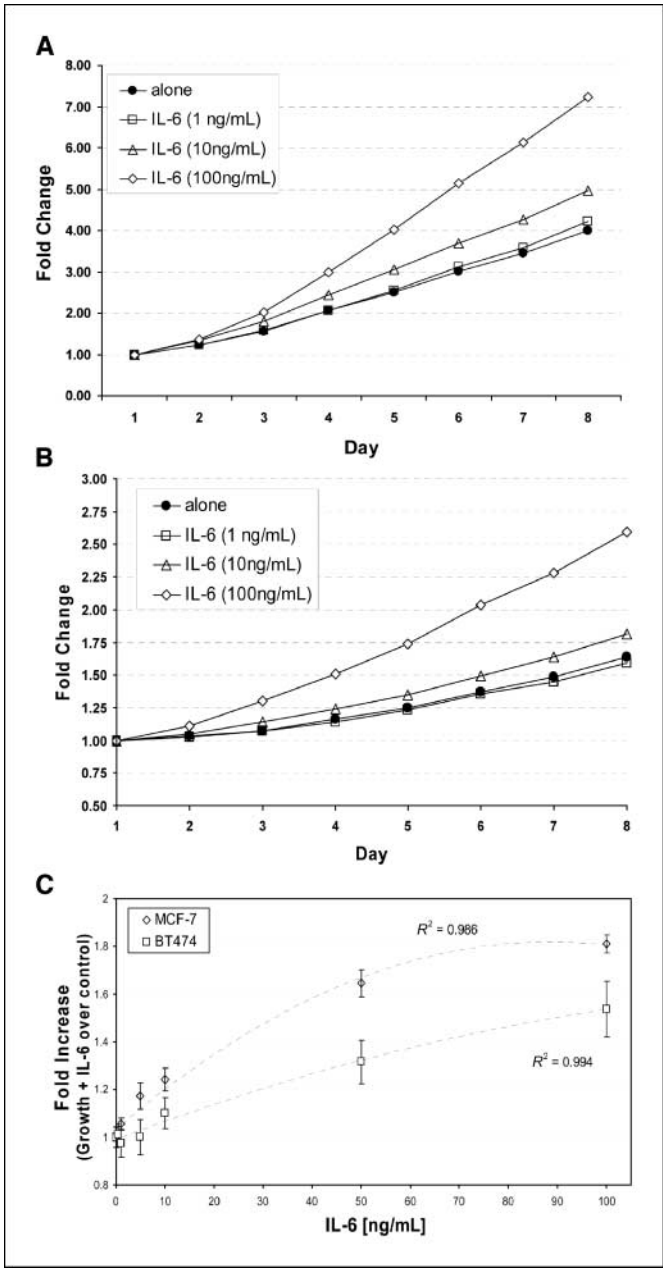


**Figure 2.** MCF-7$^{VSVgR2}$ and BT474$^{VSVgR2}$ cell growth rates increased in a dose-dependent manner when exposed to recombinant IL-6. The 3D TGA was used to assess the growth rates of MCF-7 (*A*) and BT474 (*B*) cells in the presence of serial dilutions of recombinant IL-6 (0, 1, 10, and 100 ng/mL are shown in *A* and *B*). The experiment was performed in triplicate. SDs of the MCF-7 and BT474 replicates were less than 5.0% and 7.5% for each time point. *C,* full dose-response curves at day 8 for both MCF-7 and BT474 (0, 0.5, 1, 5, 10, 50, and 100 ng/mL of IL-6).

phosphorylate STAT3 on Tyr$^{705}$ (pSTAT3$^{Y705}$) in ERα-positive breast cancer cells (13). To determine if organ-specific fibroblasts also induced pSTAT3$^{Y705}$ in an IL-6–dependent fashion, we exposed two independent ERα-positive breast cancer cell lines, MCF-7 and BT474, to conditioned medium from each of eight fibroblast lines (Fig. 1*A* and *B*). Breast, lung, and bone fibroblasts were each able to chronically induce pSTAT3$^{Y705}$, and STAT3 phosphorylation was dependent on paracrine IL-6 because removal of IL-6 from 3D Fibro-CM abrogated pSTAT3$^{Y705}$ levels (Fig. 1*A* and *B*). Consistent

with the role of IL-6 in signaling through pSTAT3$^{Y705}$ in ERα-positive breast cancer cells, induction of pSTAT3$^{Y705}$ was not observed for the skin fibroblast line CCD-39sk (Fig. 1*A* and *B*), which did not produce detectable IL-6 (Fig. 1*A*; Supplementary Fig. S1), and only a modest induction of pSTAT3$^{Y705}$ was observed for WS-1 (Fig. 1*B* and *C*), which produced minimal levels of IL-6 (Fig. 1*A*; Supplementary Fig. S1).

**IL-6 enhances the MCF-7 and BT474 growth rates in a dose-dependent manner.** To determine the specific dose-dependent growth rates of MCF-7 and BT474 in the 3D TGA, the MCF-7 and BT474 ERα-positive breast cancer cell lines were exposed to 0 to 100 ng/mL of recombinant human IL-6. Both MCF-7 and BT474 showed dose-dependent growth rate increases following exposure to 0, 1, 10, and 100 ng/mL of recombinant human IL-6 when embedded in Cultrex BME (Fig. 2*A* and *B*), and the overall growth increase for each line at day 8 within the 3D TGA was dose dependent (0, 0.5, 1, 5, 10, 50, and 100 ng/mL; Fig. 2*C*).

**Soluble human IL-6 within Fibro-CM is required for optimal growth enhancement by breast, lung, and bone fibroblasts.** To determine if organ-specific fibroblasts were equally capable of affecting breast cancer cell growth rates, we evaluated a panel of eight mesenchymal fibroblast lines isolated from four independent tissues for their ability to directly alter growth rates of the ERα-positive breast cancer cell lines MCF-7 and BT474. Breast tumor cells expressing DsRed protein were embedded in Cultrex BME alone or in the presence of conditioned medium (3D Fibro-CM) isolated from breast (BNF14 and BNF15), lung (MRC-5 and WI-38), bone (Ped300 and P162), and skin (WS-1 and CCD-39sk) cultures. MCF-7$^{VSVgR2}$ and BT474$^{VSVgR2}$ growth rates were enhanced in the presence of 3D Fibro-CM from breast fibroblasts, bone marrow fibroblasts, and lung fibroblasts (Fig. 3*A* and *B*) compared with breast cancer cell growth alone. However, cancer cell growth rates were greatly attenuated when IL-6 was immunoprecipitated from the 3D Fibro-CM (Fig. 3*A* and *B*). In contrast, skin fibroblasts (i.e., WS-1 and CCD-39sk) minimally affected breast cancer cell growth rates (Fig. 3*A* and *B*), which corresponded to their production of soluble IL-6 (Supplementary Fig. S1). These observations were limited to ERα-positive breast cancer cell lines as breast, lung, and bone fibroblasts were unable to alter the growth rate of the ERα-negative cell line MDA-MB-231 or the immortalized breast epithelial cell line MCF-10A (Supplementary Fig. S2*A* and *B*), both of which produce autocrine IL-6 (data not shown). Finally, the extent to which organ-specific fibroblast enhanced MCF-7 ($P = 0.005$) or BT474 ($P < 0.001$) growth rates directly correlated to the quantity of IL-6 secreted by each fibroblast line (Fig. 3*C* and *D*).



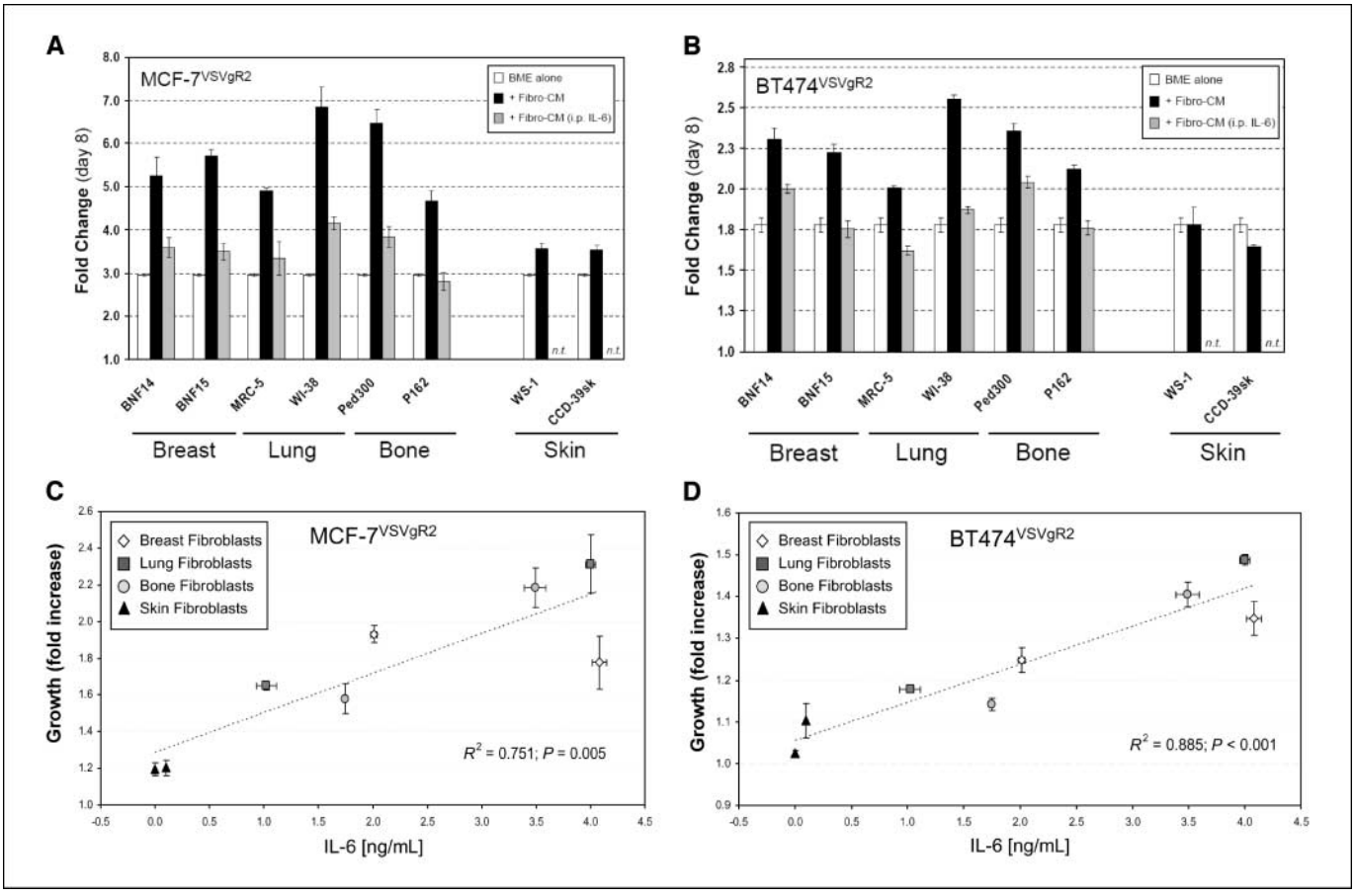


**Figure 3.** The 3D TGA was used to assess the growth rates of breast cancer cells alone and in the presence of Fibro-CM and Fibro-CM stripped of IL-6 via immunoprecipitation [*Fibro-CM (i.p. IL-6)*]. Fibroblasts from breast, lung, and bone enhanced the growth rates of MCF-7$^{VSVgR2}$ (*A*) and BT474$^{VSVgR2}$ (*B*) cells, and removal of IL-6 severely compromised the ability of Fibro-CM to enhance breast cancer cell growth rates. These data represent the values collected on day 8 of the assay from four independent experiments with each experiment run in triplicate. Increased growth rates of MCF-7 (*C*) and BT474 (*D*) breast tumor cells directly correlated to the level of soluble IL-6 produced by organ-specific fibroblasts. Breast, lung, and bone fibroblasts produce higher levels of IL-6, which directly correlated to the level of growth rate enhancement of ERα-positive breast cancer cells ($P \leq 0.005$). *n.t., not tested* (IL-6 not present).

**Senescent skin fibroblasts secrete IL-6 and enhance tumor growth rates in an IL-6–dependent manner.** Mounting evidence suggests that senescent fibroblasts promote the growth of neoplastic cells in xenografts (21–23), and inflammatory mediators can accelerate the onset of a senescent phenotype in fibroblasts (23, 43). Consistent with previous reports of inflammatory factor-induced senescence, we observed that exposure of presenescent skin fibroblasts to IL-6 (10 ng/mL) for 3 weeks accelerated the onset of a senescent phenotype, which is normally acquired after extensive *in vitro* passaging (21). IL-6–induced senescence persisted even after 1-week withdrawal of exogenous IL-6. The ensuing senescence phenotype was associated with increased expression of $p21^{Waf1}$, $p16^{INK4}$, elevated senescence-associated β-galactosidase activity, enlarged cell shape, formation of nuclear SAHF, increased culture doubling time, and reduced bromodeoxyuridine incorporation. Senescence-associated cellular changes were reproducibly detected in skin fibroblasts following chronic IL-6 exposure (Supplementary Fig. S3).

Similar to other senescent fibroblast models (44), post-IL-6–treated fibroblasts produced increased levels of IL-6 compared with controls (760 ± 91.7 pg/mL and 136.7 ± 55.1 pg/mL, respectively; $P = 0.001$, Student's $t$ test). We therefore compared the ability of IL-6–producing and IL-6–nonproducing skin fibroblasts to promote MCF-7 tumor xenograft engraftment and growth in immunocompromised mice. MCF-7 cells were injected s.c. in the presence or absence of passage-matched skin fibroblasts (i.e., IL-6–induced senescence and presenescent controls) in 18 female BALB/c nude mice. After 5 weeks, palpable MCF-7 tumors were observed in eight of nine animals coinjected with IL-6–producing skin fibroblasts, whereas no MCF-7 tumor xenografts were established in animals coinjected with MCF-7 cells and passage-matched skin fibroblasts or with MCF-7 cells alone (Fig. 4*A*). To verify that increased tumor growth was dependent on paracrine fibroblast IL-6, we compared the growth rates of the eight engrafted MCF-7 tumor xenografts (i.e., MCF-7 + IL-6–producing skin fibroblasts) following injections of human IL-6 neutralizing antibody with PBS. We observed that anti-IL-6 antibody administration resulted in a significant reduction ($P = 0.029$) of tumor xenograft growth rates over the ensuing 3-week period (Fig. 4*B* and *C*). Histologic examination of tumors at necropsy revealed a lower degree of invasive growth in anti-IL-6 antibody–treated mice compared with PBS-treated controls (Supplementary Fig. S4). These data suggest that IL-6–producing fibroblasts enhance breast cancer cell growth and invasiveness *in vivo*.

**Paracrine IL-6 promotes growth and invasion of MCF-7 tumor cells through STAT3/Notch-3/Jagged-1 and CA-IX.** We recently showed that autocrine IL-6 in MCF-7 cells enhanced growth rates through elevated Jagged-1 (14), and IL-6/Notch-3 interplay was previously reported to promote invasive characteristics of MCF-7 cells via CA-IX up-regulation (14). Here, we show that IL-6 or conditioned medium containing IL-6 induced MCF-7 invasiveness, which was attenuated by anti-IL-6 blocking antibody, Notch-3 knockdown, or CA-IX knockdown when compared with respective controls (Fig. 5*A* and *B*). Finally, we found that breast cancer–associated fibroblasts secreted increased IL-6 compared with their normal counterparts (patient 1: 128.7 + 20 versus 1,130 + 140; patient 2: 820 + 43.6 versus 2,366 + 152; $P = 0.001$) and induced a more pronounced invasive phenotype in MCF-7 cells. Again, MCF-7 invasiveness could be attenuated by administration of IL-6 neutralizing antibody or by inhibiting Notch-3 or CA-IX (Fig. 5*C*).

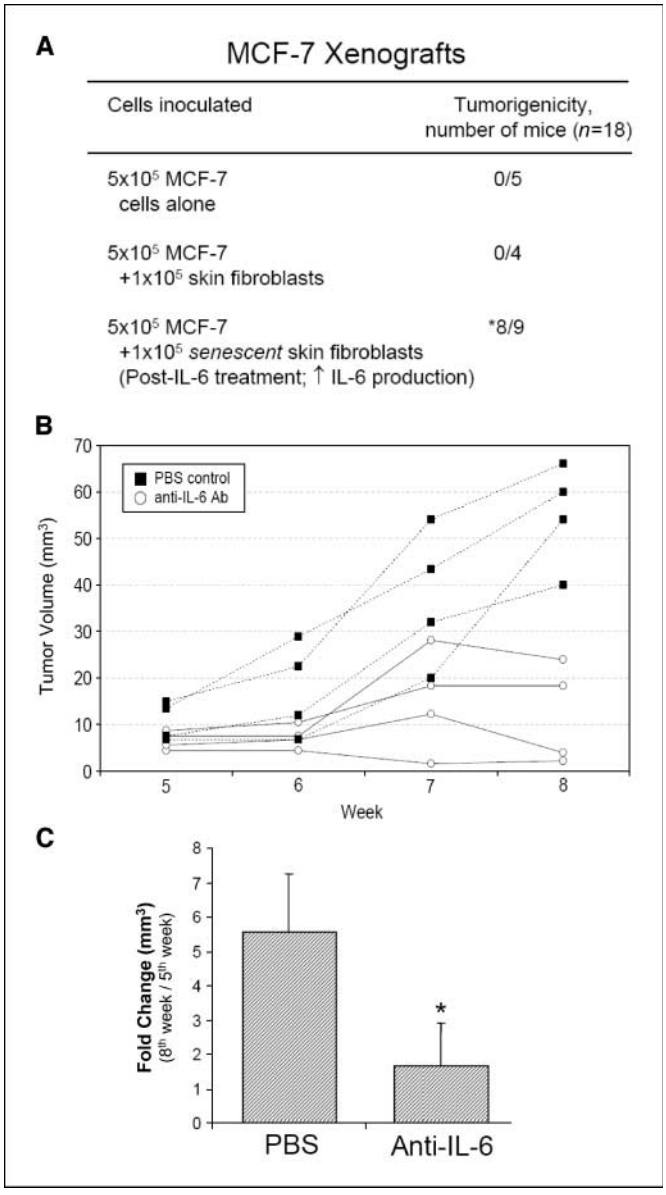


**Figure 4.** Engraftment rates and IL-6 dependency of MCF-7 xenografts in immunocompromised mice. *A,* female mice received an inoculum of $5 \times 10^5$ MCF-7 cells ± $1 \times 10^5$ primary human skin fibroblasts (presenescent or IL-6–induced senescence; see Supplementary Fig. S3), and palpable tumors were examined at 5 wk after tumor cell injection. *, eight mice harboring palpable tumors were subsequently used in *B* for anti-IL-6 antibody injections. Neutralizing IL-6 antibody significantly reduces growth and invasion of MCF-7 xenografts coinjected with IL-6–producing fibroblasts. *B,* tumor xenograft growth rates and tumor volume increases over 3-wk period in MCF-7/post-IL-6 skin fibroblast xenografts ($n = 8$). Mice were divided into two groups of four and treated s.c., near the tumor, with anti-IL-6 (100 μg) or PBS alone at 200 μL per injection every 3 d. *C,* mean changes in growth rate between the PBS and anti-IL-6 groups ($n = 4$). *, $P = 0.029$, Mann-Whitney test.

These data suggest that IL-6–producing fibroblasts promote a more severe malignant phenotype in breast cancer cells through activation of Notch-3, Jagged-1, and CA-IX, all of which lie downstream of STAT3.

## Discussion

Two studies in the early 1990s showed that engraftment and growth rates of human mammary tumor xenografts could be

enhanced by coinjecting tumor cells with fibroblasts or their soluble factors (17, 45). Yet, fibroblast-derived factor(s), which is capable of enhancing tumor growth rates, still remains largely unknown (12, 16). In this study, we showed that fibroblast production and secretion of IL-6 directly correlated with the ability of organ-specific fibroblasts to enhance ERα-positive breast cancer cell growth rates (Figs. 4 and 5) and invasion (Fig. 5). Conversely, ERα-negative breast cancer cells, such as MDA-MB-231 and MDA-MB-468, which produce autocrine IL-6, are less responsive to paracrine IL-6 signaling (Supplementary Fig. S2*A*; refs. 12, 13, 28, 46). Taken together, our data support a model whereby IL-6, through autocrine or paracrine signaling, promotes breast cancer growth and invasion through STAT3 and its downstream effectors, such as Notch-3, Jagged-1, and CA-IX (Fig. 6).

Consistent with our *in vitro* and *in vivo* data on human breast cancer cell lines (13, 28), Yashiro and colleagues (16) showed that primary breast cancer xenografts had higher engraftment rates and grew more rapidly when coinjected with patient-matched normal or cancer-associated breast fibroblasts. In addition, both we and Yashiro and colleagues (16) have shown that skin fibroblasts (i.e., presenescent) are ineffective at enhancing *in vitro* breast cancer cell growth (Fig. 3) and xenograft growth (Fig. 4*A*), respectively. Whereas Yashiro and colleagues were unable to identify a mechanism that could explain the differential growth rates of breast tumor xenografts in response to breast or skin fibroblasts, our study shows that production of paracrine IL-6 from organ-specific fibroblasts directly correlates to the level to which a specific fibroblast can enhance the growth rate of breast cancer cells (Fig. 3*C* and *D*).

Further support for our findings stems from recent studies that revealed that MCF-7 xenograft growth rates were enhanced *in vivo* when coinjected with human bone marrow–derived MSCs, whereas the growth rates of MDA-MB-231 xenografts were not (12). These observations are consistent with organ-specific fibroblast

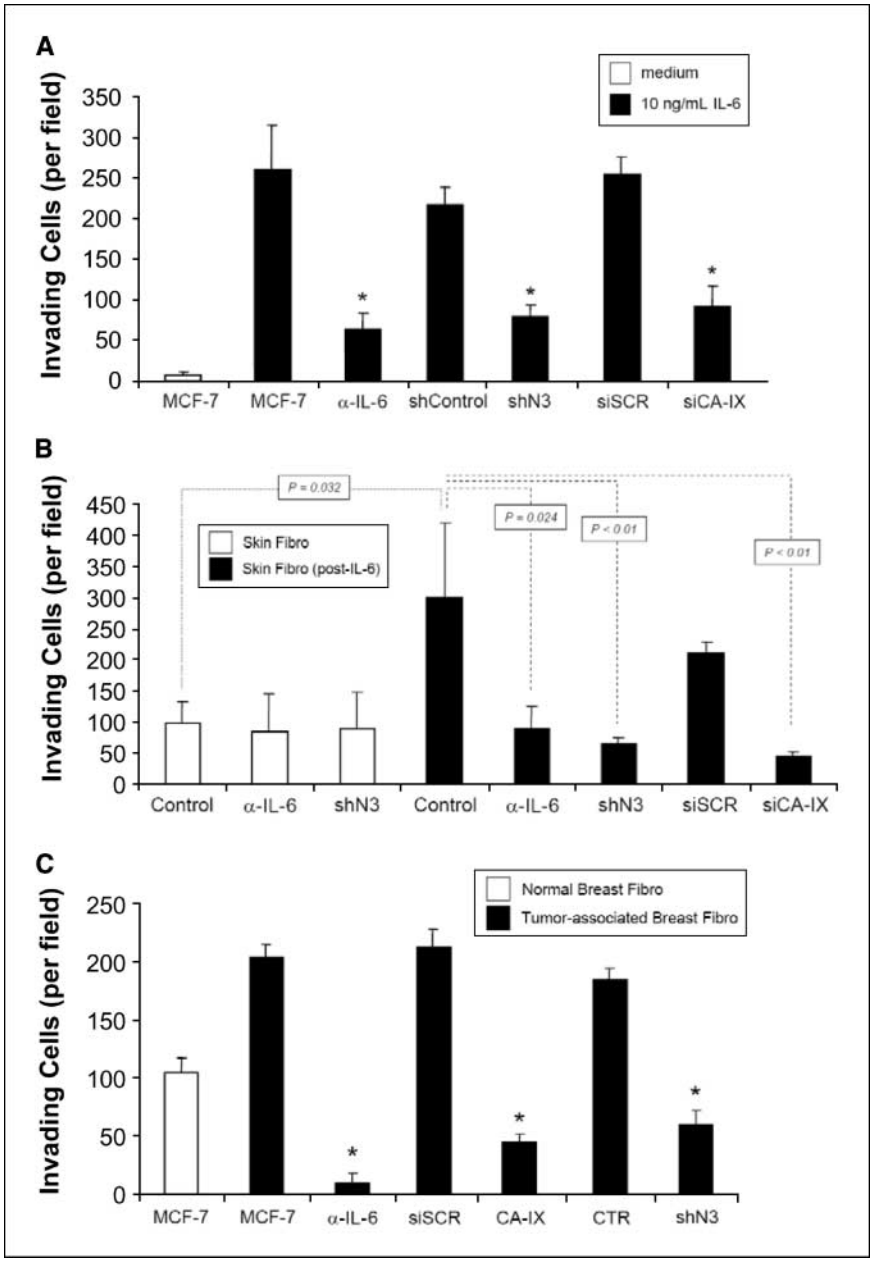


**Figure 5.** STAT3 regulates Notch-3 and CA-IX expression, which together promote IL-6–dependent MCF-7 invasion. *A,* invasion assays of MCF-7 cells exposed to IL-6 (10 ng/mL) plus neutralizing IL-6 antibody (1.5 μg/mL, 24 h), shControl, shNotch-3 (*shN3*), siScrambled (*SCR*), and siCA-IX. *, $P < 0.001$, compared with MCF-7 + IL-6 (10 ng/mL). *B,* invasion assays of MCF-7 cells exposed to supernatants of presenescent and senescent skin fibroblasts, in the presence of anti-IL-6 (1.5 μg/mL, 24 h), infected with shNotch-3/control vectors or transfected with CA-IX/control (*SCR*)–specific siRNA (*P* values shown on graph). *C,* invasion assays of MCF-7 cells exposed to supernatants from patient-matched normal and tumor-associated mammary gland fibroblasts in the presence of anti-IL-6 (1.5 μg/mL, 24 h), infected with shNotch-3/shControl vectors or transfected with CA-IX/control (*SCR*)–specific siRNA. *, $P < 0.001$, relative to "MCF-7 + tumor-associated breast fibroblasts".

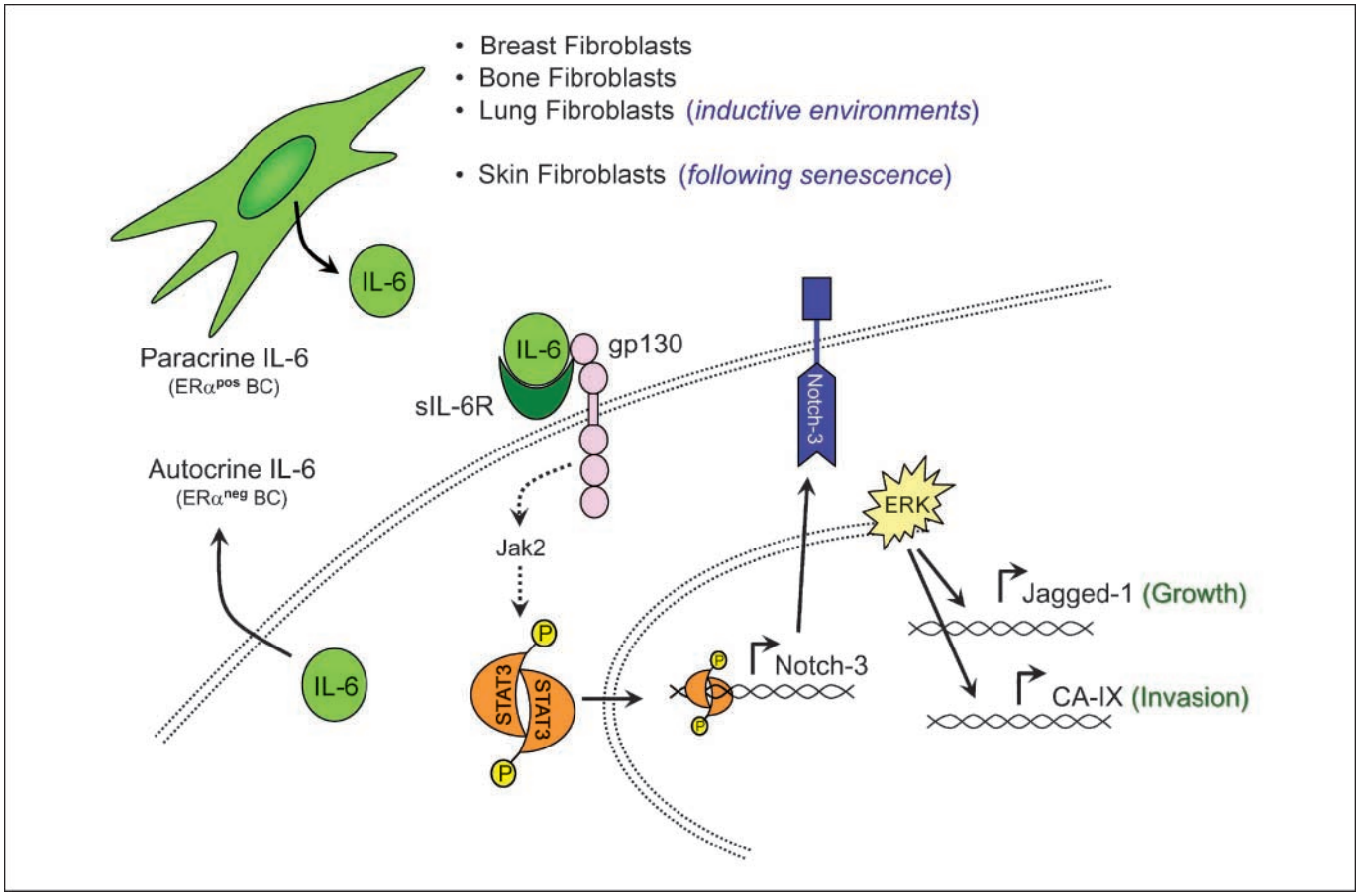


**Figure 6.** Model for enhanced breast tumor cell growth and invasion following exposure to IL-6. Breast tumor cells that fail to produce autocrine IL-6 (e.g., $ER\alpha^{pos}$) dramatically respond to paracrine IL-6 signaling from tumor stroma. In contrast, autocrine IL-6–positive breast tumor cells (e.g., $ER\alpha^{neg}$) display lower dependency on microenvironment-derived IL-6. IL-6 exposure leads to chronic induction of $STAT3^{Y705}$ through IL-6/IL-6R/gp130 and Jak2 (13, 14, 50). Chronic STAT3 activation then leads to elevated expression of Notch-3 and induction of the mitogen-activated protein kinase pathway (14). Following activation of extracellular signal-regulated kinase, expression of Jagged-1 (growth) and CA-IX (invasion) is elevated, which promotes enhanced growth and invasion of breast tumor cells.

production of IL-6 (Fig. 1) and that MDA-MB-231 cells produce autocrine IL-6 themselves (13). In fact, we found that MDA-MB-231 growth rates were unaffected by any of the eight fibroblast lines tested in this study (Supplementary Fig. S2*A*) or by MSC (13). We also examined the effect of organ-specific fibroblasts on MCF-10A growth rates, an immortalized human breast epithelial cell line. MCF-10A growth rates were unaffected by the presence of breast, lung, bone, or skin fibroblasts or their soluble factors (Supplementary Fig. S2*B*).

Although skin fibroblasts produced little to no IL-6 (Fig. 1; Supplementary Fig. S1), senescent skin fibroblasts strongly upregulated IL-6 secretion and enhanced breast cancer cell growth rates and invasion (Figs. 4 and 5). Interestingly, senescent fibroblasts are known to amplify epithelial cell aggressiveness and tumorigenesis (21–23). Senescent skin fibroblasts and breast tumor–derived fibroblasts, which produce elevated levels of IL-6, showed a similar ability to induce MCF-7 invasiveness (Fig. 5*B* and *C*). Such data are consistent with those reported for ovarian tumor–associated fibroblasts displaying senescent characteristics (23). Specifically, it was observed that ovarian fibroblasts underwent cellular senescence *in vitro* when exposed to the inflammatory chemokine GRO1, which is secreted by ovarian cancer cells (23). These data led the authors to propose that tumor-associated fibroblasts undergo senescence following chronic exposure to *in vivo* tumor environments (23). Similar to GRO1, we found that chronic exposure of low-passage skin fibroblasts to IL-6 elicits a phenotype similar to that of *in vitro* senescent fibroblasts as shown by typical markers of senescence, such as β-galactosidase, $p21^{Waf1}$, $p16^{INK4}$ gene expression, and nuclear senescence-associated heterochromatin foci (21, 47). We also showed that IL-6–exposed skin fibroblasts display an enhanced and sustained capability to secrete IL-6 and to promote the *in vivo* tumorigenic potential of MCF-7 cells (Fig. 4).

Inherent characteristics (e.g., gene expression profiles) of cancer cells or "seeds" have predictive value with regard to tissue-specific metastasis (48, 49), but little is known about characteristics of certain organs or "soils" that make them more fertile for cancer metastasis. Our data suggest that soluble factors such as IL-6, produced in a paracrine fashion by organ-specific fibroblasts, can serve as a biological "fertilizer" for Stephen Paget's permissive soils (1). Further studies will be needed to establish the extent to which inherent characteristics of unique tissues contribute to site-specific metastasis in breast cancer and how metastasis may be influenced by levels of local paracrine factors such as IL-6.

## Disclosure of Potential Conflicts of Interest

No potential conflicts of interest were disclosed.

## Acknowledgments

Received 2/1/2008; revised 7/2/2008; accepted 8/1/2008.

**Grant support:** Elsa U. Pardee Foundation (B.M. Hall), Susan G. Komen Foundation, NIH grants CA109451 and CA-116199 (F.C. Marini), RFO funds-ex 60%, and Cornelia and Robert Pallotti Foundation (M. Bonafé).

The costs of publication of this article were defrayed in part by the payment of page charges. This article must therefore be hereby marked *advertisement* in accordance with 18 U.S.C. Section 1734 solely to indicate this fact.

We thank Fondazione Cassa di Risparmio in Bologna and Fondazione del Monte in Bologna e Ravenna for supporting the Center for Applied Biomedical Research and FIRB Project.

## References

**1.** Paget S. The distribution of secondary growths in cancer of the breast. Lancet 1889;1:571–3.
**2.** Nguyen DX, Massague J. Genetic determinants of cancer metastasis. Nat Rev Genet 2007;8:341–52.
**3.** Hess KR, Pusztai L, Buzdar AU, Hortobagyi GN. Estrogen receptors and distinct patterns of breast cancer relapse. Breast Cancer Res Treat 2003;78:105–18.
**4.** James JJ, Evans AJ, Pinder SE, et al. Bone metastases from breast carcinoma: histopathological-radiological correlations and prognostic features. Br J Cancer 2003; 89:660–5.
**5.** Guy CT, Cardiff RD, Muller WJ. Induction of mammary tumors by expression of polyomavirus middle T oncogene: a transgenic mouse model for metastatic disease. Mol Cell Biol 1992;12:954–61.
**6.** Bugge TH, Lund LR, Kombrinck KK, et al. Reduced metastasis of polyoma virus middle T antigen-induced mammary cancer in plasminogen-deficient mice. Oncogene 1998;16:3097–104.
**7.** Orimo A, Gupta PB, Sgroi DC, et al. Stromal fibroblasts present in invasive human breast carcinomas promote tumor growth and angiogenesis through elevated SDF-1/CXCL12 secretion. Cell 2005;121:335–48.
**8.** Radisky DC, Levy DD, Littlepage LE, et al. Rac1b and reactive oxygen species mediate MMP-3-induced EMT and genomic instability. Nature 2005;436:123–7.
**9.** Kurose K, Hoshaw-Woodard S, Adeyinka A, Lemeshow S, Watson PH, Eng C. Genetic model of multi-step breast carcinogenesis involving the epithelium and stroma: clues to tumour-microenvironment interactions. Hum Mol Genet 2001;10:1907–13.
**10.** Moinfar F, Man YG, Arnould L, Bratthauer GL, Ratschek M, Tavassoli FA. Concurrent and independent genetic alterations in the stromal and epithelial cells of mammary carcinoma: implications for tumorigenesis. Cancer Res 2000;60:2562–6.
**11.** Djouad F, Plence P, Bony C, et al. Immunosuppressive effect of mesenchymal stem cells favors tumor growth in allogeneic animals. Blood 2003;102:3837–44.
**12.** Karnoub AE, Dash AB, Vo AP, et al. Mesenchymal stem cells within tumour stroma promote breast cancer metastasis. Nature 2007;449:557–63.
**13.** Sasser AK, Sullivan NJ, Studebaker AW, Hendey LF, Axel AE, Hall BM. Interleukin-6 is a potent growth factor for ER-α-positive human breast cancer. FASEB J 2007;21: 3763–70.
**14.** Sansone P, Storci G, Tavolari S, et al. IL-6 triggers malignant features in mammospheres from human ductal breast carcinoma and normal mammary gland. J Clin Invest 2007;117:3988–4002.
**15.** Fiebig HH, Maier A, Burger AM. Clonogenic assay with established human tumour xenografts: correlation of *in vitro* to *in vivo* activity as a basis for anticancer drug discovery. Eur J Cancer 2004;40:802–20.
**16.** Yashiro M, Ikeda K, Tendo M, Ishikawa T, Hirakawa K. Effect of organ-specific fibroblasts on proliferation and differentiation of breast cancer cells. Breast Cancer Res Treat 2005;90:307–13.
**17.** Camps JL, Chang SM, Hsu TC, et al. Fibroblast-mediated acceleration of human epithelial tumor growth *in vivo*. Proc Natl Acad Sci U S A 1990;87:75–9.
**18.** Shekhar MP, Werdell J, Santner SJ, Pauley RJ, Tait L. Breast stroma plays a dominant regulatory role in breast epithelial growth and differentiation: implications for tumor development and progression. Cancer Res 2001; 61:1320–6.
**19.** van Roozendaal CE, van Ooijen B, Klijn JG, et al. Stromal influences on breast cancer cell growth. Br J Cancer 1992;65:77–81.
**20.** Kalluri R, Zeisberg M. Fibroblasts in cancer. Nat Rev Cancer 2006;6:392–401.
**21.** Campisi J, d'Adda di Fagagna F. Cellular senescence: when bad things happen to good cells. Nat Rev Mol Cell Biol 2007;8:729–40.
**22.** Krtolica A, Parrinello S, Lockett S, Desprez PY, Campisi J. Senescent fibroblasts promote epithelial cell growth and tumorigenesis: a link between cancer and aging. Proc Natl Acad Sci U S A 2001;98:12072–7.
**23.** Yang G, Rosen DG, Zhang Z, et al. The chemokine growth-regulated oncogene 1 (Gro-1) links RAS signaling to the senescence of stromal fibroblasts and ovarian tumorigenesis. Proc Natl Acad Sci U S A 2006;103: 16472–7.
**24.** Fidler IJ. Seed and soil revisited: contribution of the organ microenvironment to cancer metastasis. Surg Oncol Clin N Am 2001;10:257–69, vii-viii.
**25.** Cukierman E, Pankov R, Stevens DR, Yamada KM. Taking cell-matrix adhesions to the third dimension. Science 2001;294:1708–12.
**26.** Ghosh S, Spagnoli GC, Martin I, et al. Three-dimensional culture of melanoma cells profoundly affects gene expression profile: a high density oligonucleotide array study. J Cell Physiol 2005;204:522–31.
**27.** Miralem T, Steinberg R, Price D, Avraham H. VEGF(165) requires extracellular matrix components to induce mitogenic effects and migratory response in breast cancer cells. Oncogene 2001;20:5511–24.
**28.** Sasser AK, Mundy BL, Smith KM, et al. Human bone marrow stromal cells enhance breast cancer cell growth rates in a cell line-dependent manner when evaluated in 3D tumor environments. Cancer Lett 2007;254:255–64.
**29.** Phillips TM, McBride WH, Pajonk F. The response of CD24(−/low)/CD44+ breast cancer-initiating cells to radiation. J Natl Cancer Inst 2006;98:1777–85.
**30.** Zhou J, Zhang H, Gu P, Bai J, Margolick JB, Zhang Y. NF-κB pathway inhibitors preferentially inhibit breast cancer stem-like cells. Breast Cancer Res Treat 2008;111: 419–27.
**31.** Heinrich PC, Behrmann I, Muller-Newen G, Schaper F, Graeve L. Interleukin-6-type cytokine signalling through the gp130/Jak/STAT pathway. Biochem J 1998; 334:297–314.
**32.** Kawano M, Hirano T, Matsuda T, et al. Autocrine generation and requirement of BSF-2/IL-6 for human multiple myelomas. Nature 1988;332:83–5.
**33.** Okamoto M, Lee C, Oyasu R. Interleukin-6 as a paracrine and autocrine growth factor in human prostatic carcinoma cells *in vitro*. Cancer Res 1997;57: 141–6.
**34.** Okada K, Shimizu Y, Nambu S, Higuchi K, Watanabe A. Interleukin-6 functions as an autocrine growth factor in a cholangiocarcinoma cell line. J Gastroenterol Hepatol 1994;9:462–7.
**35.** Ancrile B, Lim KH, Counter CM. Oncogenic Ras-induced secretion of IL6 is required for tumorigenesis. Genes Dev 2007;21:1714–9.
**36.** Knupfer H, Preiss R. Significance of interleukin-6 (IL-6) in breast cancer [review]. Breast Cancer Res Treat 2007;102:129–35.
**37.** DeMichele A, Martin AM, Mick R, et al. Interleukin-6 −174G→C polymorphism is associated with improved outcome in high-risk breast cancer. Cancer Res 2003;63: 8051–6.
**38.** Yu H, Kortylewski M, Pardoll D. Crosstalk between cancer and immune cells: role of STAT3 in the tumour microenvironment. Nat Rev Immunol 2007;7:41–51.
**39.** Ling X, Arlinghaus RB. Knockdown of STAT3 expression by RNA interference inhibits the induction of breast tumors in immunocompetent mice. Cancer Res 2005;65:2532–6.
**40.** Selander KS, Li L, Watson L, et al. Inhibition of gp130 signaling in breast cancer blocks constitutive activation of Stat3 and inhibits *in vivo* malignancy. Cancer Res 2004;64:6924–33.
**41.** Kassem M, Khosla S, Spelsberg TC, Riggs BL. Cytokine production in the bone marrow microenvironment: failure to demonstrate estrogen regulation in early postmenopausal women. J Clin Endocrinol Metab 1996;81:513–8.
**42.** Chavey C, Bibeau F, Gourgou-Bourgade S, et al. Oestrogen receptor negative breast cancers exhibit high cytokine content. Breast Cancer Res 2007;9:R15.
**43.** Moiseeva O, Mallette FA, Mukhopadhyay UK, Moores A, Ferbeyre G. DNA damage signaling and p53-dependent senescence after prolonged β-interferon stimulation. Mol Biol Cell 2006;17:1583–92.
**44.** de Magalhaes JP, Chainiaux F, de Longueville F, et al. Gene expression and regulation in $H_2O_2$-induced premature senescence of human foreskin fibroblasts expressing or not telomerase. Exp Gerontol 2004;39: 1379–89.
**45.** Noel A, De Pauw-Gillet MC, Purnell G, Nusgens B, Lapiere CM, Foidart JM. Enhancement of tumorigenicity of human breast adenocarcinoma cells in nude mice by matrigel and fibroblasts. Br J Cancer 1993;68:909–15.
**46.** Studeny M, Marini FC, Dembinski JL, et al. Mesenchymal stem cells: potential precursors for tumor stroma and targeted-delivery vehicles for anticancer agents. J Natl Cancer Inst 2004;96:1593–603.
**47.** Funayama R, Ishikawa F. Cellular senescence and chromatin structure. Chromosoma 2007;116:431–40.
**48.** Minn AJ, Gupta GP, Siegel PM, et al. Genes that mediate breast cancer metastasis to lung. Nature 2005; 436:518–24.
**49.** Minn AJ, Kang Y, Serganova I, et al. Distinct organ-specific metastatic potential of individual breast cancer cells and primary tumors. J Clin Invest 2005;115:44–55.
**50.** Berishaj M, Gao SP, Ahmed S, et al. Stat3 is tyrosine-phosphorylated through the interleukin-6/glycoprotein 130/Janus kinase pathway in breast cancer. Breast Cancer Res 2007;9:R32.